

# Topological edge states in the Su-Schrieffer-Heeger model subject to balanced particle gain and loss

Marcel Klett<sup>1,2</sup>, Holger Cartarius<sup>3</sup>, Dennis Dast<sup>1</sup>, Jörg Main<sup>1</sup>, and Günter Wunner<sup>1</sup>

<sup>1</sup> Institut für Theoretische Physik 1, Universität Stuttgart, 70550 Stuttgart, Germany

<sup>2</sup> Institut für Theoretische Physik and Center for Quantum Science, Universität Tübingen, Auf der Morgenstelle 14, 72076 Tübingen, Germany

<sup>3</sup> Physik und ihre Didaktik, Universität Stuttgart, 70550 Stuttgart, Germany

Received: date / Revised version: date

**Abstract.** We investigate the Su-Schrieffer-Heeger model in presence of an injection and removal of particles, introduced via a master equation in Lindblad form. It is shown that the dynamics of the density matrix follows the predictions of calculations in which the gain and loss are modeled by complex  $\mathcal{PT}$ -symmetric potentials. In particular it is found that there is a clear distinction in the dynamics between the topologically different cases known from the stationary eigenstates.

**PACS.** 03.65.Vf Phases: geometric; dynamic or topological – 11.30.Er Charge conjugation, parity, time reversal, and other discrete symmetries – 73.20.-r Electron states at surfaces and interfaces – 73.43.Nq Quantum phase transitions

## 1 Introduction

Today topological many-body systems are a strongly investigated topic and are in many cases well understood [1–5]. One of the best known examples is the explanation of the quantized Hall effect [6, 7] in terms of a topological invariant [8]. Of special interest are topologically protected Majorana zero modes [5, 9–12] since they are robust against local defects or disorder. Typically two topologically different phases can arise when a certain parameter of the system is varied. In the topologically nontrivial phase (TNP) energies within the band gap appear, and their corresponding eigenstates are called edge states since they appear at the edge between two different types of solids or potentials. In the topologically trivial phase (TTP) the gap closing states are absent.

Since no system is completely isolated recently the question was raised of how a coupling to the environment can influence the existence of topologically nontrivial modes and the appearance of topologically protected edge states [13–28]. Furthermore, it was shown that dissipation can even be used to create topologically nontrivial states [29, 30]. In many of these studies complex potentials were used, which provide an efficient way of introducing gain or loss to the probability amplitude in quantum mechanics [31]. With their help the time-dependent processes of a decay or growth of a state can be described by a stationary but non-Hermitian Schrödinger equation. Successful applications to describe a system coupled to an environment in this way can be found for electromagnetic

waves [32–35], electric circuits [36], optomechanics [37], and quantum mechanics [38–49].

In most studies of edge states in presence of gain or loss, particular attention was devoted to  $\mathcal{PT}$ -symmetric potentials, i.e. potentials which commute under the combined action of the parity and the time-reversal operators  $\mathcal{P}$  and  $\mathcal{T}$ , respectively.  $\mathcal{PT}$ -symmetric Hamiltonians represent a special class of operators since they allow for real energy eigenvalues and even completely real energy spectra even though they are not Hermitian. This is possible since it can be shown that an eigenvalue of a  $\mathcal{PT}$ -symmetric operator is always real if the corresponding eigenstate  $\psi$  possesses the same symmetry. If it does not, there is always a second eigenstate  $\mathcal{PT}\psi$  and the eigenvalues of these two eigenstates form a pair of complex conjugates [50]. The latter case is usually referred to as spontaneously broken  $\mathcal{PT}$  symmetry. In the case of a Hamiltonian the complex energy eigenvalues describe a growth (positive imaginary part) or decay (negative imaginary part) of the probability amplitude. The opposite case of preserved  $\mathcal{PT}$  symmetry is then related to the situation of balanced gain and loss. The in- and outfluxes are spatially separated but have the same strength. In total the state does neither decay nor grow, and this is expressed by its real energy eigenvalue. The physical reality of these relations have been proved experimentally in optics [51–53], however, proposals also exist for Bose-Einstein condensates in quantum mechanics [54–57].

Together with the Kitaev chain [58] the Su-Schrieffer-Heeger (SSH) model [59] stands in the main focus when

the relation between  $\mathcal{PT}$  symmetry and topologically protected edge states is investigated. In these models two completely different behaviors were observed. While in the Kitaev chain it was found that the  $\mathcal{PT}$  symmetry is protected within the TNP when a non-Hermitian potential is applied [23, 24], the opposite was revealed for the SSH model developed for the description of the conducting organic material polyacetylene. Its  $\mathcal{PT}$ -symmetry is instantaneously broken within the TNP as soon as gain and loss via a  $\mathcal{PT}$ -symmetric potential are introduced [21, 22]. This can be explained by the different symmetries of the edge states [60]. However, in a modification of the SSH model new edge states possessing an additional symmetry could be exploited to experimentally prove the presence of unbroken  $\mathcal{PT}$  symmetry in optics [61].

The application of complex potentials always means a restriction to an effective description. The potentials act on the probability amplitude of each particle to be in the system under consideration [42]. A common and more realistic way of handling environment effects in many-body systems is the solution of the dynamics using Lindblad master equations [62]. With this description a statistical addition or removal of whole particles is implemented. It could be shown that this approach is strongly related to complex  $\mathcal{PT}$ -symmetric potentials in sufficiently large systems. For a description of Bose-Einstein condensates with balanced gain and loss of single particles the mean-field limit is a  $\mathcal{PT}$ -symmetric Gross-Pitaevskii equation [63]. It has been shown that the topological phases can still be distinguished when information is extracted from a density matrix resulting from a master equation and that they can remain robust against certain couplings to the environment [64, 65].

In our work we want to address a different question. The purpose of this paper is to gain insight into the relation of the complex potential introduced above with the description of particle in- and outcouplings via master equations. The statistical process introduced in the master equation typically leads to a crucially different behavior. As soon as the assumption of smooth gain-loss potentials is violated, in particular in presence of quantum fluctuations, the stability of  $\mathcal{PT}$ -symmetric states gets destroyed as was discussed in optics [66]. As mentioned above, for bosonic systems a strong relation between both approaches could be established. This, however, is possible only in the mean-field limit [63]. In the present case we are far away from this limit, and the temporal evolution of single particles matters. Thus, we cannot expect that the topological properties of the description with complex potentials should transfer to the master equation approach. In this paper we find that, yet, the relation still is very strong.

We investigate this point for the SSH model subject to balanced gain and loss of particles at different lattice sites. The master equation is formulated in such a way that it corresponds to the  $\mathcal{PT}$ -symmetric potentials used in previous studies [21, 60], in which it was shown that the topological edge states break the potential's  $\mathcal{PT}$  symmetry. This should be observable in the dynamics of the

master equation via a survival or decay of an initial occupation of the states. We show that the dynamics follows the predictions of the stationary calculations accessible in the effective non-Hermitian approach. In addition, it is possible to see clear differences in the outcome of the dynamics in cases which correspond to either the TTP or the TNP in the stationary model. All in all the results indicate that the observations in the stationary model lead to valuable answers.

We first introduce our model in Sec. 2. Then, in Sec. 3.1, we study the dynamics of the closed system without addition or removal of particles. This provides the basis for understanding the dynamics in presence of particle gain and loss in Sec. 3.2. The results of the master equation are compared to the predictions of stationary calculations with complex potentials in Sec. 3.3. Concluding remarks are given in Sec. 4.

## 2 Model and methods

We consider a one-dimensional case with a lattice distance  $a = 1$  and a total of  $N$  lattice sites. The system under investigation is the Su-Schrieffer-Heeger model, of which the Hamiltonian in terms of the fermionic creation (annihilation) operators  $c_i^\dagger$  ( $c_i$ ) reads [59]

$$H_{\text{SSH}} = \sum_n \left( t_- c_{2n-1}^\dagger c_{2n} + t_+ c_{2n}^\dagger c_{2n+1} + \text{h.c.} \right), \quad (1)$$

where  $t_\pm = t(1 \pm \Delta \cos \Theta)$  contains the hopping amplitude  $t$  and the dimerization strength  $\Delta \cos \Theta$ , which can vary from  $-\Delta$  to  $\Delta$ .

We will investigate the system under environment effects in such a way that it can exchange particles (electrons) with the environment at both ends of the chain. In accordance with [63] this is done with a master equation for the density operator  $\varrho$  in Lindblad form,

$$\partial_t \varrho = -i[H_{\text{SSH}}, \varrho] + L_+(\varrho) + L_-(\varrho). \quad (2)$$

The superoperators read

$$L_-(\varrho) = -\frac{\gamma}{2} (c_1^\dagger c_1 \varrho + \varrho c_1^\dagger c_1 - 2c_1 \varrho c_1^\dagger), \quad (3)$$

$$L_+(\varrho) = -\frac{\gamma}{2} (c_N c_N^\dagger \varrho + \varrho c_N c_N^\dagger - 2c_N^\dagger \varrho c_N), \quad (4)$$

where we assume that the possibility to take a particle out of the system at the first site is the same as the probability of injecting a particle at the last site of the chain. The strength of the in- and outcoupling effect is described by  $\gamma$ .

To solve the Lindblad master equation (2) a quantum Monte-Carlo approach is used [67], for which the Hamiltonian has to be represented in matrix form. This limits the size of the accessible Fock space. However, since the goal of this paper is a comparison of the results of the Lindblad master equations with those of a non-Hermitian stationary calculation, which addresses a single-particle problem [21, 22, 60], we restrict the system to the case that

only a single particle is present on the lattice. To obtain a quantity comparable to the occupation probabilities of the stationary calculations we calculate the mean value of the particle number operator at each site,

$$\langle n_i(t) \rangle = \langle \rho(t) n_i \rangle, \quad (5)$$

where  $i$  is the index of the lattice site. Since the master equation is a statistical approach and we are interested in a relation to an effective stationary method we introduce, in addition, a temporal mean value defined as

$$\langle n_i \rangle_T = \frac{1}{s} \sum_{j=0}^s \langle n_i(t_j) \rangle \quad (6)$$

for the particle number operators  $n_i$ . The averaging is done over a time span  $T$  discretized in  $s$  equal time steps.

### 3 Dynamics

#### 3.1 Dynamics of the closed system

To be able to identify signatures of the edge states in the presence of gain and loss we first investigate their visibility in dynamical calculations of the closed system. Thus, we neglect the coupling to the environment in this section, i.e.,  $\gamma = 0$ . In this case the topological phase transition point in the limit of an infinite lattice size  $N \rightarrow \infty$  can be calculated analytically using the Zak-phase [68]. The transition point between the TNP and the TTP only depends on the dimerization strength and is  $\Theta = \pi/2$ . For lower values of  $\Theta$  the system is in the TNP, for higher values only topologically trivial states appear.

The Lindblad master equation is a first-order differential equation, and thus we need an initial state for our calculations. In our study the initial states are chosen as eigenstates of the time-independent single-particle problem [60]. Since we are mainly interested in the different topological phases of the SSH model we use the two edge states and one randomly chosen bulk state as starting points of the temporal evolution. The initial states are calculated in the TNP since the edge states are only visible within this parameter regime. Note that this means that the states are not in all cases stationary states of the system with the given parameters. This is not necessary for our investigation, since we are only interested in the differences that appear in the temporal evolution in the two topologically different regimes.

To distinguish the different topological phases of the SSH model we perform the time evolution of the Lindblad master equation for two different values of the dimerization strength. Figure 1 shows the example for the TTP with the value  $\Theta = 0.9\pi$ . The three initial states mentioned above are shown in the left column. The final state corresponding to the initial condition can be found next to it in the right column. What is shown is the temporal mean value from Eq. (6). In all three cases one can observe that the states change under the evolution. This is

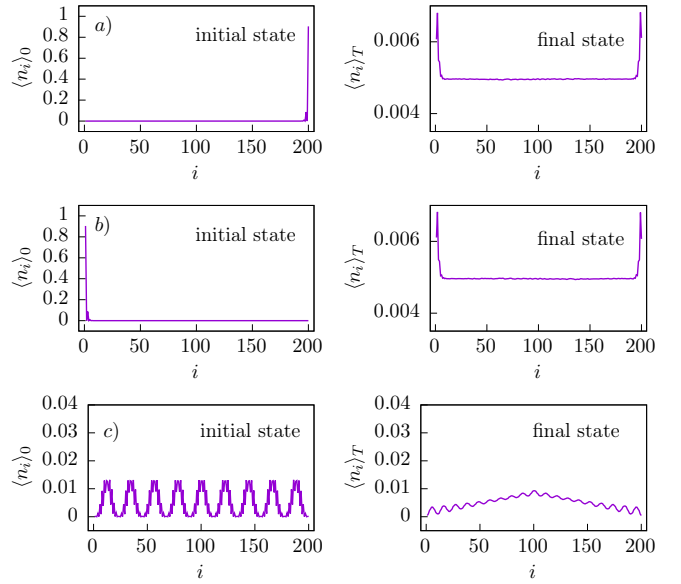


**Fig. 1.** Initial (left column) and corresponding final states (right column) for a temporal evolution in the SSH model without external gain and loss effects. The dimerization angle has a value of  $\Theta = 0.9\pi$ , and thus the system is in the topologically trivial phase, in which edge states do not exist. The calculation is carried out with the parameters  $N = 200$ ,  $t = 1.0$ , and  $\Delta = 0.3$ , and the time for the evolution is  $T = 25000$ .

expected since, as mentioned above, they are not stationary states of the system for this value of  $\Theta$ . The important observation is that all states obtain a bulk character after the evolution. In the two cases in which the edge states are used as initial conditions, a slight predominance of the occupation probability at *both* edges seems to appear. However, this has to be compared to a broad and almost uniform distribution of the probability on all lattice sites. In this respect the excess at the edges is small. The initial bulk distribution involves into a different one.

To observe the differences the behavior of the time evolution has to be compared with that in the TNP, which is shown for  $\Theta = 0.1\pi$  in Fig. 2. The initial states are the same as in Fig. 1. After the time evolution they show a structure that clearly differs from the previous case. The initial edge states almost retain their shape. A few lattice sites in the vicinity of the edges grow in intensity and the edge site itself becomes slightly damped. However, each of the initial edge states remains clearly located at *one* edge. The initial bulk state evolves into almost the same state as in the TTP.

The study so far already gives us a hint that it is possible to distinguish the TTP and the TNP from the dynamics of different initial states. To obtain an even deeper insight we plot in Fig. 3 the occupation of the last 1, 3, 5, and 20 lattice sites after the temporal evolution as a function of the dimerization angle  $\Theta$ . In all cases the initial state is the edge state localized at the end of the chain, i.e. that in the first row of Fig. 1. After the time evolution of  $T = 25000$  time units the temporal average (6) shows the same results in all four cases. For dimerization angles

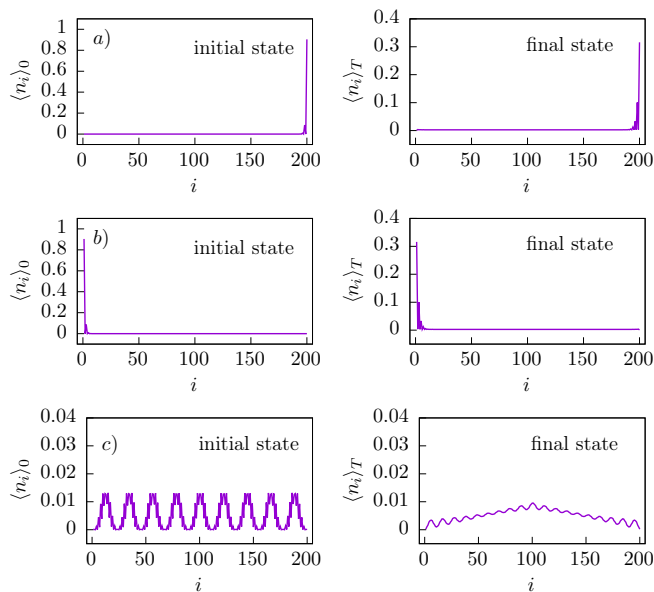


**Fig. 2.** Initial (left column) and final states (right column) for a temporal evolution in the SSH model without external gain and loss effects. With the dimerization angle  $\Theta = 0.1\pi$  the system is in the topologically nontrivial phase. The remaining parameters are the same as in Fig. 1.

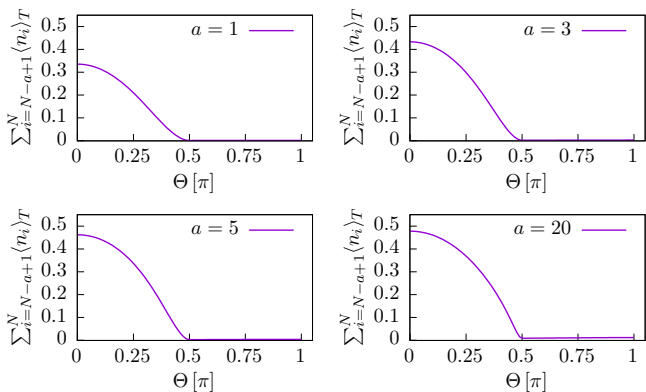


**Fig. 3.** Mean value of the occupation of the last  $a$  lattice sites in dependence of the dimerization angle  $\Theta$  without gain and loss. The analytical topological phase transition point in the case of  $N \rightarrow \infty$  is at  $\Theta = \pi/2$ . One can clearly see that around the analytical phase transition point the amplitude of finding a particle at the edge is drastically reduced as compared to the TNP. It stays almost constant beyond the transition point. The parameters are  $\Delta = 0.3$ ,  $t = 1.0$ , and  $N = 1000$ . The time evolution is done for  $T = 25000$ . In all cases the initial state has a distribution mainly localized at the right edge, see figure 1 (a).

$\Theta \lesssim \pi/2$  we find a nonvanishing occupation at the edges, which shrinks to almost zero as  $\Theta$  approaches  $\pi/2$ . For larger values of  $\Theta$  the occupation remains constant at a very low level. At the critical dimerization strength a sharp kink is visible. In the case  $N \rightarrow \infty$  the topological phase transition is exactly at  $\Theta = \pi/2$ . Thus, the sharp kink is the signature we search for the identification of the topo-

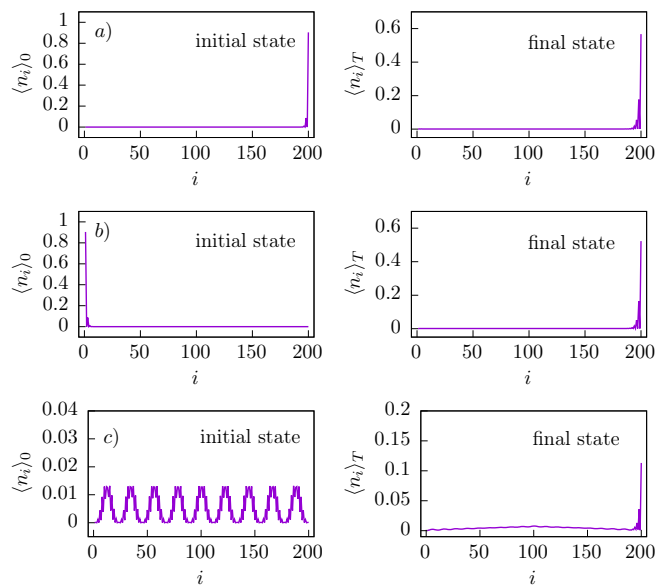


**Fig. 4.** Initial (left column) and final states (right column) as in Fig. 2 with nonvanishing gain and loss effect  $\gamma = 0.1$ . With the dimerization angle  $\Theta = 0.1\pi$  the system is in the topologically nontrivial phase. The parameters are  $N = 200$ ,  $t = 1.0$  and  $\Delta = 0.3$ . The time for the evolution is  $T = 25000$ . Dominated by the edge state coupling to the influx of particles the particle predominantly occupies the right edge for all initial distributions.

logical phase transition in a dynamical calculation that is also feasible with in- and outfluxes of particles.

### 3.2 Dynamics in presence of particle gain and loss

With the method used in the previous section we can turn to the case of particle gain and loss, i.e. we set  $\gamma = 0.1$  and solve the Lindblad master equation (2). An example for the TNP is shown in Fig. 4. As expected for the topologically nontrivial phase edge features are clearly visible. However, it is always the same edge state which dominates the evolution independent of the initial state. This is not surprising since the lattice site with the highest occupation is the last one, i.e. that with gain (cf. Eq. (4)). As is known from the stationary calculation with complex potentials [21, 60] the edge states of the SSH model break the  $\mathcal{PT}$  symmetry of the Hamiltonian, and thus they cannot exist as stationary states. They will either gain or lose in amplitude, depending on whether the amplification or the damping lattice site prevails. Since the initial states chosen in Fig. 4 are no eigenstates of the system there is always an overlap with the growing state, and thus it will dominate every temporal evolution. This is what is observed in the figure.

Since the amplification is obviously the most significant effect seen in Fig. 4 and only the site with particle gain stands out one might conclude that the existence of topologically nontrivial states cannot be identified as soon as the gain effect is present. If a site with gain exists and is

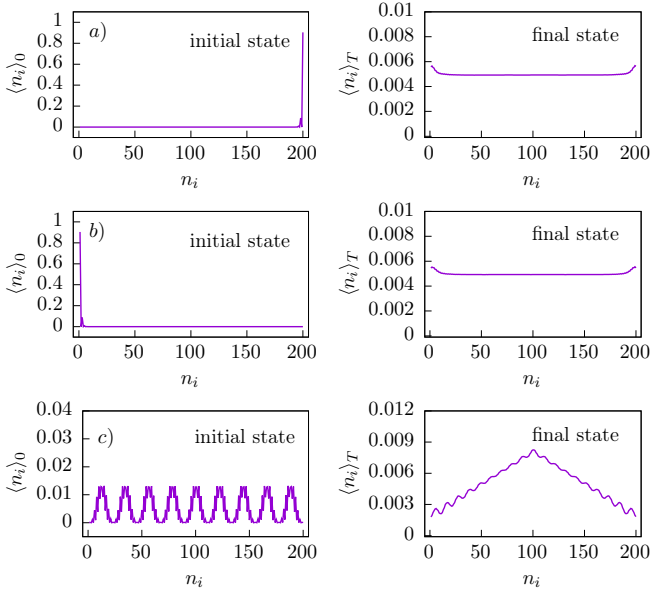


**Fig. 5.** Initial (left column) and final states (right column) in the case of gain and loss for  $\gamma = 0.1$  and a dimerization angle of  $\Theta = 0.9\pi$ , i.e. the system is in the topologically trivial phase. The remaining parameters are the same as in Fig. 4. Since there are no  $\mathcal{PT}$ -broken edge states in the TTP the time averaged occupation ends up in a broad and symmetric bulk distribution.

occupied (or disproportionately highly occupied as compared to loss sites due to an asymmetry) it can be expected to dominate the whole dynamics. This should give rise to a large occupation at the edge that is not distinguishable from an edge state. But this assumption turns out to be wrong. The TTP with the same gain and loss strength is shown in Fig. 5, in which a clear difference to Fig. 4 is visible. Now the dynamics ends up in a bulk state for all initial states. For both edge states the same final distribution is obtained. There are still slightly higher occupations at the edges than in the center of the bulk, but they are drastically weaker as compared to the Hermitian case (cf. Fig. 1).

The missing dominance of the edge states can be explained in a simple way. From the stationary calculation we know that they are the first states breaking the  $\mathcal{PT}$  symmetry, and for the chosen  $\gamma = 0.1$  they are even the only states for which gain and loss are not balanced. Consequently, in the TTP, in which no edge states are present, the whole spectrum consists of states experiencing a unitary time evolution. Any initial state can be decomposed into these stationary states and will undergo oscillations with constant total amplitude. The time average of these oscillations assumes the symmetric distributions visible in Fig. 5. Thus, it is the strong relation of the edge states to  $\mathcal{PT}$ -symmetry breaking in the SSH model, which introduces a pronounced difference in the dynamics.

Since the presence of the edge states has a strong influence on the dynamics, they also have a significant impact on the time averaged occupation at the right edge as can be seen in Fig. 6. For the initial state shown on the left,

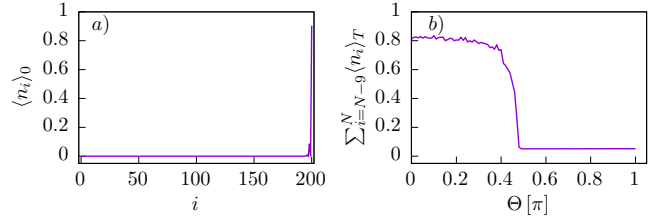


**Fig. 6.** Mean value b) of the occupation of the last 10 lattice sites in dependence of the dimerization angle  $\Theta$  in presence of gain and loss with the value  $\gamma = 0.1$ . The initial state is shown in a). The remaining parameters are  $\Delta = 0.3$ ,  $t = 1.0$ , and  $N = 1000$ . The time evolution is done for  $T = 25000$ . In comparison to the case without gain and loss the kink in the edge occupation is much more pronounced, cf. Fig. 3.

the time averaged mean occupation of the last 10 lattice sites is drawn on the right as a function of  $\Theta$ . The result is similar to that in Fig. 3. However, the kink at the topological phase transition is much sharper. Thus, it still clearly identifies the topological phase transition. It appears just below  $\Theta = \pi/2$ , i.e. at the point, where it also appears in the case without in- and outcoupling of particles.

### 3.3 Comparison to the stationary non-Hermitian approach

An important question in this study is the comparability of the results of the non-hermitian stationary calculation using complex potentials [21,60] with the more realistic in- and outcoupling of particles described by Lindblad master equations. The procedure used in this paper was capable of identifying the appearance of edge states, and thus of distinguishing the two topological phases. From the stationary calculations it is known that topologically non-trivial edge states can be found even in the presence of gain and loss effects, and the phase transition point is not affected by gain and loss acting on the edge sites [21,60]. The same is now found in the dynamical calculations with master equations. The difference to the analytical value  $\Theta = \pi/2$  can be traced back to the finite lattice size.

The agreement between both approaches goes even beyond the pure existence of the edge states for the same values of the dimerization angle  $\Theta$ . The dynamics of the master equations follows exactly the predictions that can be done by looking at the existence or nonexistence of complex energy eigenstates in the stationary picture. This turned out to be valuable in the explanation of the final states in Sec. 3.2. The influence of the complex energy eigenstates is clearly present.

## 4 Conclusion

We studied the SSH model with gain and loss at the edges, which was introduced via Lindblad master equations. This description is more realistic than that of previous studies using effective complex  $\mathcal{PT}$ -symmetric potentials [21,60]. We found that the addition and removal

of particles does not destroy the existence of two distinct topological phases identified by the existence of edge states. These edge states could be detected in the dynamics by studying time-averaged occupation probabilities of the individual lattice sites. This is in very good agreement with calculations of the stationary Schrödinger equation in presence of complex potentials.

The agreement goes even further. The dynamical predictions of the energy eigenvalues of the stationary approach, which are real in the case of  $\mathcal{PT}$ -symmetric states and complex for broken  $\mathcal{PT}$  symmetry, can be clearly observed in the evolution of the density operator using the master equations. The study shows that both approaches agree very well. In the investigation of Bose-Einstein condensates it was shown that a Gross-Pitaevskii equation with complex potentials is the exact mean-field limit of a many-particle description, in which gain and loss are implemented via Lindblad master equations [63, 69]. In this study we have found that even if both approaches act on the individual particles, a good agreement is found, and thus the application of complex potentials in many works dealing with topological condensed matter models subject to gain and loss [13–15, 17, 19–24] is justified.

The identification of the two different topological phases is already very clear by investigating the dynamics. However, one certainly is interested in finding a more direct method by directly determining a topological invariant [29, 65, 70, 71]. Thus, a natural next step is the extension of the formalism in such a way that a topological invariant, e.g. an extended complex Zak phase, can be obtained. In addition, the current study was restricted to the single-particle case. In presence of gain the particle number can in principle change. Thus, it would be interesting to see how the system behaves if more particles can enter. This would be of crucial importance for bosons, which can occupy the site with gain in large numbers, and thus easily introduce instabilities in the dynamics.

## Acknowledgements

We acknowledge financial support from the Deutsche Forschungsgemeinschaft (DFG) through ZUK 63.

## Author contribution statement

All authors contributed equally to this work

## References

1. M. Z. Hasan and C. L. Kane. *Colloquium: Topological insulators*. *Rev. Mod. Phys.*, 82:3045–3067, 2010.
2. Jason Alicea. New directions in the pursuit of Majorana fermions in solid state systems. *Rep. Prog. Phys.*, 75(7):076501, 2012.
3. Alexander Altland and Martin R. Zirnbauer. Nonstandard symmetry classes in mesoscopic normal-superconducting hybrid structures. *Phys. Rev. B*, 55:1142–1161, 1997.
4. Andreas P. Schnyder, Shinsei Ryu, Akira Furusaki, and Andreas W. W. Ludwig. Classification of topological insulators and superconductors in three spatial dimensions. *Phys. Rev. B*, 78:195125, 2008.
5. Martin Leijnse and Karsten Flensberg. Introduction to topological superconductivity and Majorana fermions. *Semicond. Sci. Technol.*, 27(12):124003, 2012.
6. K. v. Klitzing, G. Dorda, and M. Pepper. New method for high-accuracy determination of the fine-structure constant based on quantized Hall resistance. *Phys. Rev. Lett.*, 45:494–497, 1980.
7. Klaus von Klitzing. The quantized Hall effect. *Rev. Mod. Phys.*, 58:519–531, 1986.
8. D. J. Thouless, M. Kohmoto, M. P. Nightingale, and M. den Nijs. Quantized Hall conductance in a two-dimensional periodic potential. *Phys. Rev. Lett.*, 49:405–408, 1982.
9. V. Mourik, K. Zuo, S. M. Frolov, S. R. Plissard, E. P. A. M. Bakkers, and L. P. Kouwenhoven. Signatures of Majorana fermions in hybrid superconductor-semiconductor nanowire devices. *Science*, 336:1003–1007, 2012.
10. T. D. Stanescu and S. Tewari. Majorana fermions in semiconductor nanowires: fundamentals, modeling, and experiment. *J. Phys.: Condens. Matter*, 25(23):233201, 2013.
11. Steven R. Elliott and Marcel Franz. Colloquium: Majorana fermions in nuclear, particle, and solid-state physics. *Rev. Mod. Phys.*, 87:137–163, 2015.
12. Alexander Carmele, Markus Heyl, Christina Kraus, and Marcello Dalmonte. Stretched exponential decay of Majorana edge modes in many-body localized Kitaev chains under dissipation. *Phys. Rev. B*, 92:195107, 2015.
13. Yi Chen Hu and Taylor L. Hughes. Absence of topological insulator phases in non-hermitian  $\mathcal{PT}$ -symmetric hamiltonians. *Phys. Rev. B*, 84:153101, 2011.
14. Kenta Esaki, Masatoshi Sato, Kazuki Hasebe, and Mahito Kohmoto. Edge states and topological phases in non-hermitian systems. *Phys. Rev. B*, 84:205128, 2011.
15. Pijush K. Ghosh. A note on the topological insulator phase in non-hermitian quantum systems. *J. Phys.: Condens. Matter*, 24(14):145302, 2012.
16. O. Viyuela, A. Rivas, and M. A. Martin-Delgado. Thermal instability of protected end states in a one-dimensional topological insulator. *Phys. Rev. B*, 86:155140, 2012.
17. Henning Schomerus. Topologically protected midgap states in complex photonic lattices. *Opt. Lett.*, 38(11):1912–1914, 2013.
18. A. Rivas, O. Viyuela, and M. A. Martin-Delgado. Density-matrix Chern insulators: Finite-temperature generalization of topological insulators. *Phys. Rev. B*, 88:155141, 2013.
19. Julia M. Zeuner, Mikael C. Rechtsman, Yonatan Plotnik, Yaakov Lumer, Stefan Nolte, Mark S. Rudner, Mordechai Segev, and Alexander Szameit. Observation of a topological transition in the bulk of a non-hermitian system. *Phys. Rev. Lett.*, 115:040402, 2015.
20. C. Yuce. Topological phase in a non-hermitian symmetric system. *Phys. Lett. A*, 379(1819):1213 – 1218, 2015.
21. Baogang Zhu, Rong Lü, and Shu Chen.  $\mathcal{PT}$  symmetry in the non-hermitian Su-Schrieffer-Heeger model with complex boundary potentials. *Phys. Rev. A*, 89:062102, 2014.
22. Cem Yuce.  $\mathcal{PT}$  symmetric Floquet topological phase. *Eur. Phys. J. D*, 69(7):184, 2015.

23. Xiaohui Wang, Tingting Liu, Ye Xiong, and Peiqing Tong. Spontaneous  $\mathcal{PT}$ -symmetry breaking in non-hermitian Kitaev and extended Kitaev models. *Phys. Rev. A*, 92:012116, 2015.
24. C. Yuce. Majorana edge modes with gain and loss. *Phys. Rev. A*, 93:062130, 2016.
25. Mónica Benito, Michael Niklas, Gloria Platero, and Sigmund Kohler. Edge-state blockade of transport in quantum dot arrays. *Phys. Rev. B*, 93:115432, 2016.
26. Michael Niklas, Mónica Benito, Sigmund Kohler, and Gloria Platero. Transport, shot noise, and topology in ac-driven dimer arrays. *Nanotechnology*, 27(45):454002, 2016.
27. N. Sedlmayr, M. Fleischhauer, and J. Sirker. Fate of dynamical phase transitions at finite temperatures and in open systems. *Phys. Rev. B*, 97:045147, 2018.
28. N. Sedlmayr, P. Jaeger, M. Maiti, and J. Sirker. Bulk-boundary correspondence for dynamical phase transitions in one-dimensional topological insulators and superconductors. *Phys. Rev. B*, 97:064304, 2018.
29. C.-E. Bardyn, M. A. Baranov, C. V. Kraus, E. Rico, A. Imamoglu, P. Zoller, and S. Diehl. Topology by dissipation. *New J. Phys.*, 15(8):085001, 2013.
30. Pablo San-Jose, Jorge Cayao, Elsa Prada, and Ramón Aguado. Majorana bound states from exceptional points in non-topological superconductors. *Sci. Rep.*, 6:21427, 2016.
31. Nimrod Moiseyev. *Non-Hermitian Quantum Mechanics*. Cambridge University Press, Cambridge, 2011.
32. Shachar Klaiman, Uwe Günther, and Nimrod Moiseyev. Visualization of branch points in  $\mathcal{PT}$ -symmetric waveguides. *Phys. Rev. Lett.*, 101:080402, 2008.
33. Jan Wiersig. Enhancing the sensitivity of frequency and energy splitting detection by using exceptional points: Application to microcavity sensors for single-particle detection. *Phys. Rev. Lett.*, 112:203901, 2014.
34. S. Bittner, B. Dietz, H. L. Harney, M. Miski-Oglu, A. Richter, and F. Schäfer. Scattering experiments with microwave billiards at an exceptional point under broken time-reversal invariance. *Phys. Rev. E*, 89:032909, 2014.
35. Jörg Doppler, Alexei A. Mailybaev, Julian Böhm, Ulrich Kuhl, Adrian Girschik, Florian Libisch, Thomas J. Milburn, Peter Rabl, Nimrod Moiseyev, and Stefan Rotter. Dynamically encircling an exceptional point for asymmetric mode switching. *Nature*, 537(7618):76–79, 2016.
36. T. Stehmann, W. D. Heiss, and F. G. Scholtz. Observation of exceptional points in electronic circuits. *J. Phys. A*, 37(31):7813, 2004.
37. H. Xu, D. Mason, Luyao Jiang, and J. G. E. Harris. Topological energy transfer in an optomechanical system with exceptional points. *Nature*, 537(7618):80–83, 2016.
38. W. D. Heiss. Phases of wave functions and level repulsion. *Eur. Phys. J. D*, 7(1):1, 1999.
39. A. I. Magunov, I. Rotter, and S. I. Strakhova. Laser-induced continuum structures and double poles of the S-matrix. *J. Phys. B*, 34(1):29, 2001.
40. O. Latinne, N. J. Kylstra, M. Dörr, J. Purvis, M. Terao-Dunseath, C. J. Joachain, P. G. Burke, and C. J. Noble. Laser-induced degeneracies involving autoionizing states in complex atoms. *Phys. Rev. Lett.*, 74(1):46, 1995.
41. E. Hernández, A. Jáuregui, and A. Mondragán. Non-hermitian degeneracy of two unbound states. *J. Phys. A*, 39(32):10087, 2006.
42. Eva-Maria Graefe, Hans Jürgen Korsch, and Astrid Elisa Niederle. Quantum-classical correspondence for a non-hermitian Bose-Hubbard dimer. *Phys. Rev. A*, 82:013629, 2010.
43. R. Lefebvre, O. Atabek, M. Šindelka, and N. Moiseyev. Resonance coalescence in molecular photodissociation. *Phys. Rev. Lett.*, 103(12):123003, 2009.
44. Holger Cartarius and Nimrod Moiseyev. Fingerprints of exceptional points in the survival probability of resonances in atomic spectra. *Phys. Rev. A*, 84(1):013419, 2011.
45. W. D. Heiss, H. Cartarius, G. Wunner, and J. Main. Spectral singularities in  $\mathcal{PT}$ -symmetric Bose-Einstein condensates. *J. Phys. A*, 46(27):275307, 2013.
46. T. Gao, E. Estrecho, K. Y. Bliokh, T. C. H. Liew, M. D. Fraser, S. Brodbeck, M. Kamp, C. Schneider, S. Hofling, Y. Yamamoto, F. Nori, Y. S. Kivshar, A. G. Truscott, R. G. Dall, and E. A. Ostrovskaya. Observation of non-hermitian degeneracies in a chaotic exciton-polariton billiard. *Nature*, 526(7574):554–558, 2015.
47. Henri Menke, Marcel Klett, Holger Cartarius, Jörg Main, and Günter Wunner. State flip at exceptional points in atomic spectra. *Phys. Rev. A*, 93:013401, 2016.
48. Lukas Schwarz, Holger Cartarius, Günter Wunner, Walter Dieter Heiss, and Jörg Main. Fano resonances in scattering: An alternative perspective. *Eur. Phys. J. D*, 69(8), 2015.
49. Nikolas Abt, Holger Cartarius, and Günter Wunner. Supersymmetric model of a Bose-Einstein condensate in a  $\mathcal{PT}$ -symmetric double-delta trap. *Int. J. Theor. Phys.*, 54(11):4054–4067, 2015.
50. Carl M. Bender. Making sense of non-hermitian hamiltonians. *Rep. Progr. Phys.*, 70(6):947, 2007.
51. Christian E. Rüter, Konstantinos G. Makris, Ramy El-Ganainy, Demetrios N. Christodoulides, Mordechai Segev, and Detlev Kip. Observation of parity-time symmetry in optics. *Nat. Phys.*, 6:192, 2010.
52. Bo Peng, Sahin Kaya Ozdemir, Fuchuan Lei, Faraz Monifi, Mariagiovanna Gianfreda, Gui Lu Long, Shanhui Fan, Franco Nori, Carl M. Bender, and Lan Yang. Parity-time-symmetric whispering-gallery microcavities. *Nat. Phys.*, 10(5):394–398, 2014.
53. A. Guo, G. J. Salamo, D. Duchesne, R. Morandotti, M. Volatier-Ravat, V. Aimez, G. A. Siviloglou, and D. N. Christodoulides. Observation of  $\mathcal{PT}$ -symmetry breaking in complex optical potentials. *Phys. Rev. Lett.*, 103:093902, 2009.
54. Eva-Maria Graefe. Stationary states of a  $\mathcal{PT}$  symmetric two-mode Bose-Einstein condensate. *J. Phys. A*, 45(44):444015, 2012.
55. Fabian Single, Holger Cartarius, Günter Wunner, and Jörg Main. Coupling approach for the realization of a  $\mathcal{PT}$ -symmetric potential for a Bose-Einstein condensate in a double well. *Phys. Rev. A*, 90:042123, 2014.
56. Manuel Kreibich, Jörg Main, Holger Cartarius, and Günter Wunner. Realizing  $\mathcal{PT}$ -symmetric non-hermiticity with ultracold atoms and hermitian multiwell potentials. *Phys. Rev. A*, 90:033630, 2014.
57. Robin Gutöhrlein, Jan Schnabel, Ibrokchim Iskandarov, Holger Cartarius, Jörg Main, and Günter Wunner. Realizing  $\mathcal{PT}$ -symmetric BEC subsystems in closed hermitian systems. *J. Phys. A*, 48(33):335302, 2015.
58. A. Yu. Kitaev. Unpaired Majorana fermions in quantum wires. *Sov. Phys.-Usp.*, 44:131, 2001.

59. W. P. Su, J. R. Schrieffer, and A. J. Heeger. Solitons in polyacetylene. *Phys. Rev. Lett.*, 42:1698–1701, 1979.
60. Marcel Klett, Holger Cartarius, Dennis Dast, Jörg Main, and Günter Wunner. Relation between  $\mathcal{PT}$ -symmetry breaking and topologically nontrivial phases in the Su-Schrieffer-Heeger and Kitaev models. *Phys. Rev. A*, 95:053626, 2017.
61. S. Weimann, M. Kremer, Y. Plotnik, Y. Lumer, S. Nolte, K. G. Makris, M. Segev, M. C. Rechtsman, and A. Szameit. Topologically protected bound states in photonic parity-time-symmetric crystals. *Nat. Mater.*, 16(4):433–438, 2017.
62. Heinz-Peter Breuer and Francesco Petruccione. *The Theory of Open Quantum Systems*. Oxford University Press, Oxford, 2002.
63. Dennis Dast, Daniel Haag, Holger Cartarius, and Günter Wunner. Quantum master equation with balanced gain and loss. *Phys. Rev. A*, 90:052120, 2014.
64. O. Viyuela, A. Rivas, and M. A. Martin-Delgado. Uhlmann phase as a topological measure for one-dimensional fermion systems. *Phys. Rev. Lett.*, 112:130401, 2014.
65. D. Linzner, L. Wawer, F. Grusdt, and M. Fleischhauer. Reservoir-induced Thouless pumping and symmetry-protected topological order in open quantum chains. *Phys. Rev. B*, 94:201105, 2016.
66. Henning Schomerus. Quantum noise and self-sustained radiation of  $\mathcal{PT}$ -symmetric systems. *Phys. Rev. Lett.*, 104:233601, 2010.
67. Klaus Mølmer, Yvan Castin, and Jean Dalibard. Monte Carlo wave-function method in quantum optics. *J. Opt. Soc. Am. B*, 10(3):524–538, 1993.
68. J. Zak. Berry’s phase for energy bands in solids. *Phys. Rev. Lett.*, 62:2747–2750, 1989.
69. Dennis Dast, Daniel Haag, Holger Cartarius, Jörg Main, and Günter Wunner. Stationary states in the many-particle description of Bose-Einstein condensates with balanced gain and loss. *Phys. Rev. A*, 96:023625, 2017.
70. Simon Lieu. Topological phases in the non-hermitian Su-Schrieffer-Heeger model. *Phys. Rev. B*, 97:045106, 2018.
71. Marcel Wagner, Felix Dangel, Holger Cartarius, Günter Wunner, and Jörg Main. Numerical calculation of the complex Berry phase in non-hermitian systems. *Acta Polytech.*, 57(6):470–476, 2017.